Journal of Alloys and Compounds 521 (2012) 60–65

Contents lists available at SciVerse ScienceDirect

Journal of Alloys and Compounds

journal homepage: www.elsevier.com/locate/jallcom

Synthesis, characterization and thermal stability of a crystalline niobium oxysulfate

Qi Wang, Heng Jiang*, Hong Gong, Gang Chu, Cuihua Lin, Xiaole Dong

School of Chemistry & Material Science, Liaoning Shihua University, Fushun 113001, China

ARTICLE INFO

Article history:
Received 23 July 2011
Received in revised form 5 January 2012
Accepted 5 January 2012
Available online 14 January 2012

Keywords:
Niobium oxysulfate
Concentrated sulfuric acid
Niobium oxide
Thermal stability

ABSTRACT

The reaction of Nb_2O_5 with 96% H_2SO_4 was studied at 200–300 °C for 3 h. No reaction occurred at 200 °C. An amorphous niobium oxysulfate was formed when the reaction temperature was 250 °C. However, the crystaline niobium oxysulfate was produced when the temperature reached 300 °C. XRD analysis shows that the crystal form of the product is stable when it is calcinated at 550 °C. The product almost completely decomposed to Nb_2O_5 when the calcination temperature reached 750 °C. TG analyses show that a 23.05% mass loss is observed from 560 to 850 °C, due to the release of SO_3 and the formation of Nb_2O_5. The chemical formula of the product was estimated as $Nb_2O_4(SO_4)$ by the results of TG analysis. The product $Nb_2O_4(SO_4)$ has a different crystal form compared with the reported β-$Nb_2O_4(SO_4)$ (JCPDs 16-671). Based on powder XRD analysis, it was found that the compound crystallizes in the orthorhombic system with a space group *Pmma* (no. 51), and the corresponding lattice parameters were calculated. The crystal form was estimated as a single-crystal and multcrystalline with sizes in the micron range by SEM and TEM analysis. The molar ratio of H_2SO_4 to Nb_2O_5 (4.8:1–120.7:1) and reaction time (3–20 h) did not make any difference for the reaction at 300 °C.

1. Introduction

Metal oxysulfates (e.g. the vanadyl oxysulfate, lanthanide oxysulfate and magnesium oxysulfate) is well known as excellent materials due to their unique properties and potential applications. There are many valuable applications of metal oxysulfates in modern science and technology, for instance, the efficient catalysts, optical properties, semiconductors, dopants of phosphorescent materials, oxygen storage materials, reinforcing agents and flame retardant products, etc. [1–12].

Niobium compounds cover a large class of diverse materials whose applications include: catalysts [13–15], photoluminescence [16], microwave dielectric ceramics [17–25]. However, only limited work focused on the structure of $Nb_2O_4(SO_4)$ [26]. There was even much less work on the preparation of $Nb_2O_4(SO_4)$. There was only the β-type crystal offered in the crystallographic database, the crystal system and space group were all unknown.

The method for the preparation of niobium oxysulfate compounds was carried out by reacting Nb_2O_5 with concentrated H_2SO_4 or pyrosulfate. Successive stages and possible products were first summarized by Goroshchenko [27] as below:

$$Nb_2O_5 + H_2SO_4 \rightarrow Nb_2O_4(SO_4) + H_2O \quad (1)$$

$$Nb_2O_4(SO_4) + H_2SO_4 \rightarrow Nb_2O_3(SO_4)_2 + H_2O \quad (2)$$

$$Nb_2O_3(SO_4)_2 + H_2SO_4 \rightarrow Nb_2O_2(SO_4)_3 + H_2O \quad (3)$$

$$Nb_2O_2(SO_4)_3 + H_2SO_4 \rightarrow Nb_2O(SO_4)_4 + H_2O \quad (4)$$

$$Nb_2O(SO_4)_4 + H_2SO_4 \rightarrow Nb_2(SO_4)_5 + H_2O \quad (5)$$

Reactions (1) and (2) could occurred in aqueous solution, forming two stable sulfates $Nb_2O_4(SO_4)$ and $Nb_2O_3(SO_4)_2$. However, the product $Nb_2O(SO_4)_4$ can only be formed in non-aqueous media in reaction (4). The product $Nb_2(SO_4)_5$ in reaction (5) has not been reported ever before.

Goroshchenko and Andreeve repeated the above experiments under the conditions of different temperatures (100, 150 and 200 °C) and different concentrations of SO_3 (equivalent to 12.25–110.25 wt% of H_2SO_4) [28]. The formula of the gelatinous solid obtained at 100 °C was expressed as $2Nb_2O_5{\cdot}xSO_3{\cdot}yH_2O$. The solid consist of various products, i.e., $Nb_2O_4(SO_4)$, $Nb_2O_3(SO_4)_2$, $Nb_2O_2(SO_4)_3$ and $Nb_2O(SO_4)_4$, due to the different reaction temperatures and relative concentrations of SO_3. The β form of $Nb_2O_4(SO_4)$ was obtained, however, it is different with Ref. [27].

The density of $Nb_2O_3(SO_4)_2$ with orthorhombic structure is 3.418 g/mL [27]. Accompanied by the release of SO_3, $Nb_2O_4(SO_4)$ and Nb_2O_5 could be formed when $Nb_2O_3(SO_4)_2$ was heated from 539 to 665 °C. Land et al. prepared $Nb_2O_3(SO_4)_2$ by evaporating the mixed solution of Nb_2O_5 and H_2SO_4 [26], however, the density of $Nb_2O_3(SO_4)_2$ is 3.124 g/mL. According to TG and DSC

* Corresponding author. Tel.: +86 413 6860790; fax: +86 413 6860790.
E-mail address: hjiang78@hotmail.com (H. Jiang).

0925-8388/$ – see front matter © 2012 Elsevier B.V. All rights reserved.
doi:10.1016/j.jallcom.2012.01.033

measurements, it can be concluded that 90% of $Nb_2O_3(SO_4)_2$ was decomposed to Nb_2O_5 and SO_3 at 743 °C and the second weightlessness occurred at 838 °C which is much higher than 665 °C reported in Ref. [27].

Nb (+V) in solution was the niobium oxysulfates in the form of $Nb_2O_3(SO_4)_2$ and $Nb_2O_4(SO_4)$. The blue precursor was prepared by boiling the mixture of the metal Nb (2.0 g) and concentrated H_2SO_4 (200 mL) at 338 °C, and then the precursor was washed by the ethanol and distilled water to get $Nb_2O_3(SO_4)_2{\cdot}0.25H_2O$ [29]. Through heating 1.000 g Nb_2O_5 (3.762 mmol) and 100 mL concentrated H_2SO_4 (96%) at 300 °C, $Nb_2O_3(SO_4)_2{\cdot}0.25H_2O$ can be obtained by washing with distilled water after separating and filtering the colorless product [30]. Betke and Wickleder synthesized by $Nb_2O_2(SO_4)_3$ single crystal reacting $NbCl_5$ with fuming sulfuric acid [31]. Ra'ad et al. studied the reaction of $K_2S_2O_7$ and Nb_2O_5 at high temperatures [32]. The product obtained was determined as β-$Nb_2O_4(SO_4)$ if the molar ratio of Nb_2O_5 to $K_2S_2O_7$ was 8:5 at 450 °C, however, this synthetic method cannot be repeated.

Although niobium oxysulfate has been reported in the above literature, there are obscure descriptions and inconsistent views such as synthetic method and thermal stability. In this paper, the product was prepared by reacting Nb_2O_5 with concentrated H_2SO_4 at 300 °C (lower than the b.p. 338 °C of H_2SO_4). The chemical formula of the product was estimated as $Nb_2O_4(SO_4)$ by TG analysis. The decomposition temperature is lower than 665 °C (Ref. [27]) and 743 °C (Ref. [26]), and its XRD pattern is different with the reported β-$Nb_2O_4(SO_4)$.

2. Experimental

2.1. Material characterization

FTIR spectrum was obtained in KBr discs on a Perkin-Elmer Spectrum GX. Eight scans were co-added with a resolution of 4 cm^{-1}, in the range of 4000–400 cm^{-1}. TG analysis was carried out on a Perkin-Elmer Pyris 1 TGA. The atmosphere was air with a flow rate of 20 mL/min at 20 K/min in the range from 30 to 800 °C. X-ray powder diffraction patterns were obtained with a D/max-RB diffractometer in the 2θ range using graphite monochromated Cu Kα radiation (40 kV, 100 mA). The step scan mode was performed with a step width of 0.02 °C, at a rate of 4° (2θ) per min. The morphologies were observed using a scanning electron microscope (SEM) (JSM-7500F-EDS). High resolution morphology and selected-area electron diffraction (SAED) were performed using a transmission electron microscopy (TEM) JEOL-2100 operating at 200 kV. After crushed in ethanol, the samples were dispersed on a carbon-coated copper grid for TEM observation. X-ray photoelectron spectroscopy (XPS) analyses were performed in a Thermo Multilab 2000 spectrometer using Mg Kα (1253.6 eV) radiation. The binding energy scale was calibrated using C 1s line of aliphatic carbon, set at 284.6 eV.

2.2. Material preparation

Typical procedures are as follows: 40 mL H_2SO_4 (96%) was added to a quartz crucible containing 20 g (0.075 mol) Nb_2O_5 (99.5%, AR.) under stirring at the room temperature. The heating procedure was performed in two steps. Firstly, the mixture were heated from room temperature to 200 °C with a heating rate of 10 K/min and then held 5 min at 200 °C. Secondly, heating from 200 to 300 °C with 5 K/min and then held 3 h at 300 °C. The prepared sample was diluted with large amount of water and the supernatant was discarded after settlement for several hours. The precipitate was filtered and washed with distilled water several times. The filtrate was tested with $BaCl_2$ solution until there was no observation of $BaSO_4$ precipitation. The filter cake was dried at 65 °C for 12 h. The sample obtained is referred to as S300.

3. Results and discussion

3.1. Characterization of S300

The XRD patterns of S300 calcinated at 200 °C, 550 °C, 650 °C and 750 °C for 3 h are investigated (Fig. 1). The XRD patterns of S300 calcinated at 200–550 °C are consistent with that of the as-prepared S300. However, all the diffraction patterns of the as-prepared S300 disappear and new peaks are observed when the temperature is higher than 550 °C. The pattern at 650 °C is the mixture of Nb_2O_5 and small amount of S300. As it is shown in Fig. 1, the pattern

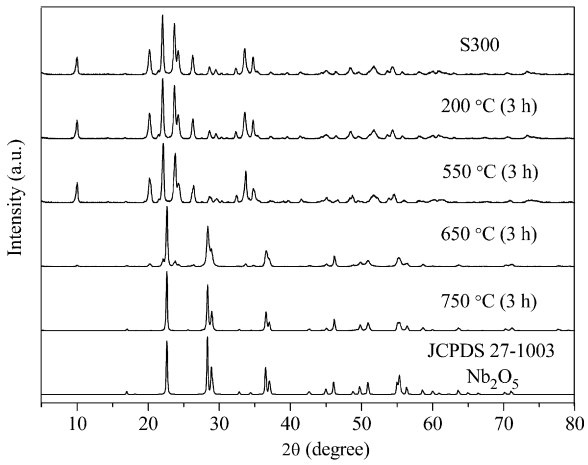

Fig. 1. XRD patterns of the S300 calcinated at different temperatures for 3 h. As a reference, the pattern of standard JCPDs 27-1003 (Nb_2O_5) is shown at the bottom.

at 750 °C is well-crystallized Nb_2O_5. It is clear that the pattern matches well with the standard JCPDs 27-1003 (Nb_2O_5) when S300 was calcinated at 750 °C.

The FTIR spectra of S300 calcinated at 200, 550, 650 and 750 °C are shown in Fig. 2. It can be seen from Fig. 2a–c, the spectra of

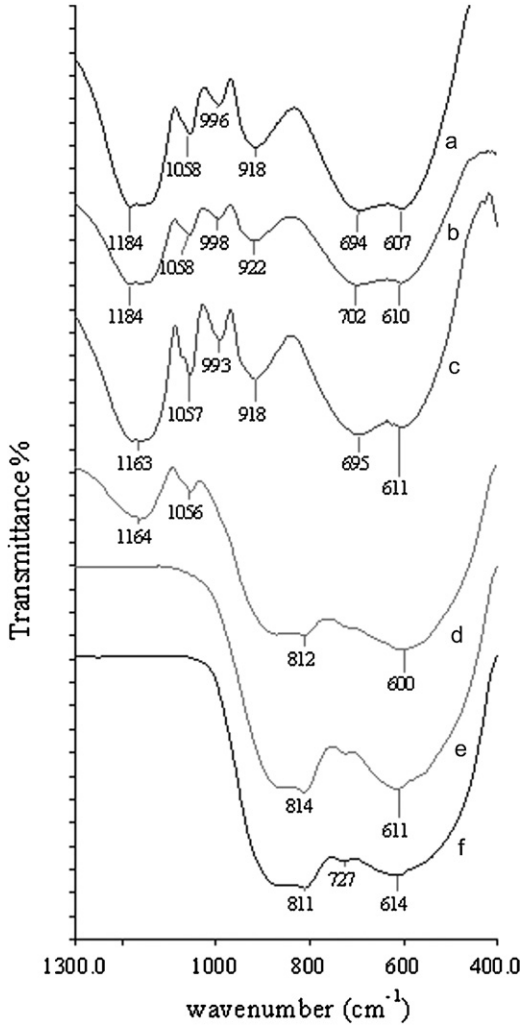

Fig. 2. FTIR spectra of S300 calcinated at different temperatures for 3 h (a, S300; b, 200 °C; c, 550 °C; d, 650 °C; e, 750 °C; f, pure Nb_2O_5).

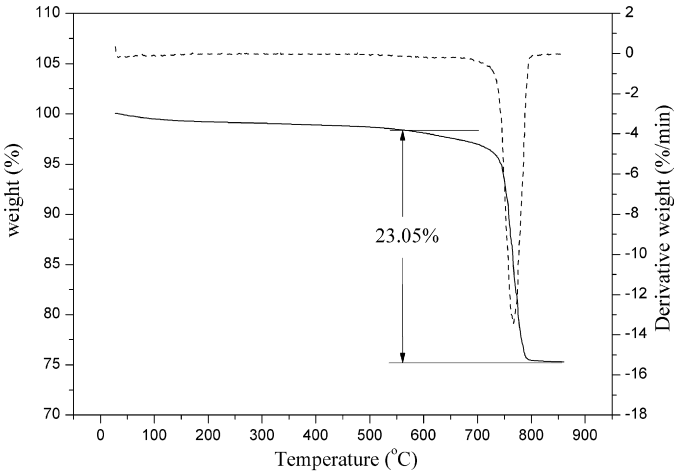

Fig. 3. TG and DTG curves of S300.

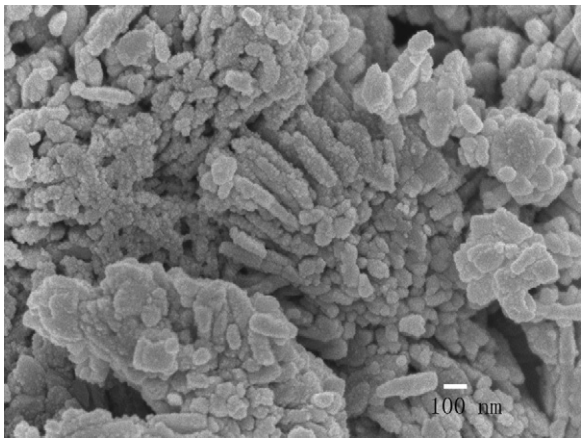

Fig. 5. Scanning electron micrograph of S300.

the sample calcinated at 200 and 550 °C is similar with that of as-prepared S300. A few weak bonds in S300 disappear, and the absorption peaks of Nb_2O_5 become more apparent when the temperature is increased to 650 °C. It can be seen from Fig. 2e and f that the SO_4^{2-} peaks disappear and all the peaks are consistent with the Nb_2O_5. It is observed that the S300 almost completely decomposes at 750 °C. These results agree well with the above XRD analyses.

Summing up, S300 is stable when the temperature is below at about 550 °C. It almost completely decomposes to Nb_2O_5 when the temperature reached 750 °C.

The TG and DTG curves of the as-prepared S300 are presented in Fig. 3. The first mass loss step occurs within the temperature range of 30 °C to 400 °C. This initial mass loss is attributed to the removal of small amount of water. The second decomposition step shows a 23.05% mass loss from 560 to 850 °C, in which stage SO_3 was released and the residue of Nb_2O_5 was formed at about 750 °C. The formula of S300 could be hypothesized as $Nb_2O_x(SO_4)_{5-x}$. According to the 23.05% weight loss due to the release of SO_3, it can be calculated that x is 4.01. So the chemical formula of S300 is estimated as $Nb_2O_4(SO_4)$.

The symmetry of the SO_4^{2-} ion is approximately T_d. When SO_4^{2-} coordinates to a metal, its symmetry is lowered and marked changes in the spectrum are expected because of changes in the selection rules. The degenerate vibrations split when SO_4^{2-} coordinates to a metal, which may be act as unidentate, chelating bidentate or bridging bidentate ligands [33]. As shown in Fig. 2a, bands within the range from 900 to 1200 cm^{-1} are the significant feature of SO_4^{2-}. In Fig. 2a, ν_1 appears with medium intensity, ν_3 splits into three bands (996, 1057 and 1180 cm^{-1}). These results suggest that the symmetry is further lowered to C_{2v}. Thus the SO_4^{2-} group in this complex is concluded to be chelating bidentate or bridging bidentate ligands. The SO_4^{2-} group in S300 can be estimated as bridging bidentate ligand because the maximum absorption peak is less than 1200 cm^{-1} [34–36]. Compared with Fig. 2f, the Nb—O and Nb═O stretching of Nb_2O_5 shifted to low-frequency region because of the present of SO_4^{2-}, as shown in Fig. 2a.

3.1.1. XRD analysis of S300

As shown in Fig. 4, the main peaks due to S300 are 10°, 20.2°, 22°, 23.6°, 24.2°, 26.2°, 28.6°, 33.5°, 34.7°, 48.3°, 51.8° and 54.3°, respectively. The standard XRD patterns of β-$Nb_2O_4(SO_4)$ are 20.5°, 22.7°, 24.5°, 26.7°, 29°, 34.1°, 35.4°, 49.2°, 52.2°, 54.8°, 60°, 61.7°, 63.7°, 67.9°, 71.2° and 73.9°, respectively. It can be seen from Fig. 4 that there are not any diffraction patterns at about 10° for the standard XRD patterns of β-$Nb_2O_4(SO_4)$. Furthermore, all the diffraction patterns attributed to S300 shift to the lower 2θ values at the range from 20 to 60° compared with that of JCPDs 16-671. There are not obvious diffraction patterns from 60 to 80° in the XRD patterns of S300. It can be confirmed that the XRD patterns of S300 are lack of conformity with those of standard JCPDs 16-671 (β-$Nb_2O_4(SO_4)$).

X-ray powder diffraction intensities for structural determination were collected at 298 K with a step-scan technique in a 2θ range from 5° to 118° with a fixed counting time (t) of 15 s/step

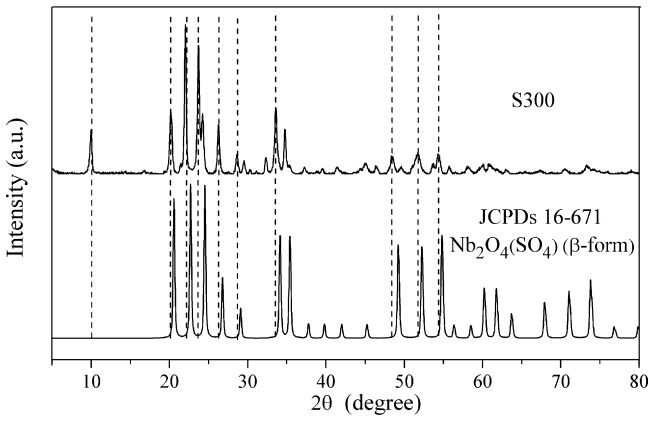

Fig. 4. XRD patterns of S300. As a reference, the pattern of standard JCPDs 16-671 (β-$Nb_2O_4(SO_4)$) is shown at the bottom.

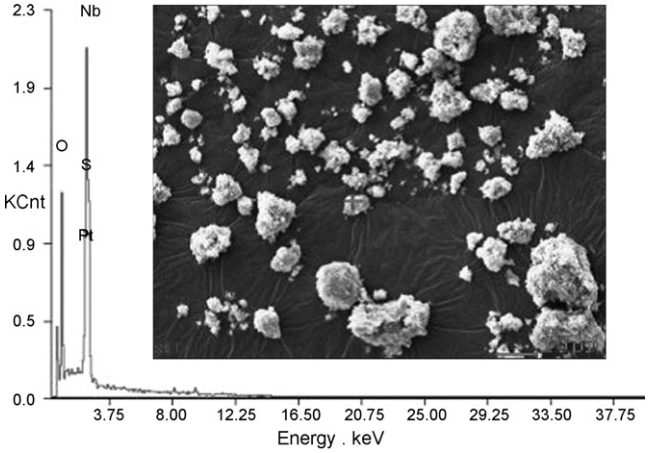

Fig. 6. EDS spectrum of S300 coated with platinum.

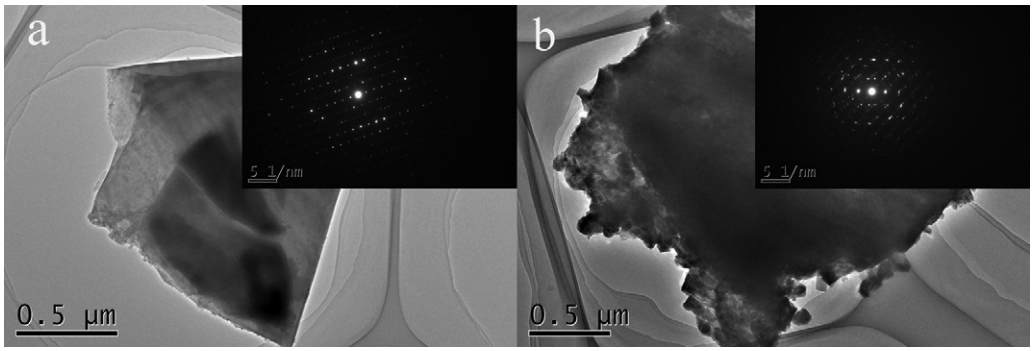

Fig. 7. TEM micrograph and SAED pattern of S300.

and a step interval ($\Delta 2\theta$) of 0.02°. Peak positions were determined after Kα2 stripping on a computer program POWDERX, followed by the indexing procedure on a computer program TREOR90. Table 1 presents the details of the crystal data information for $Nb_2O_4(SO_4)$. The metric of the unit cell suggested an orthorhombic setting with $a \neq b \neq c$ and $\alpha = \beta = \gamma = 90°$. $Nb_2O_4(SO_4)$ crystallizes in the orthorhombic with space group *Pmma* (no. 51) and contains four formula units in the unit cell.

Table 1
Crystallographic data of $Nb_2O_4(SO_4)$.

Chem formula	$Nb_2O_4(SO_4)$
Mol wt (g/mol)	345.89
a (Å)	17.643
b (Å)	5.273
c (Å)	6.567
V (Å^3)	610.9
Z	4
Space group	*Pmma* (no. 51)
Crystal system	Orthorhombic
D_{calc} (g/cm^3)	3.760

3.1.2. SEM-EDS investigations

The morphology of the S300 was observed by SEM (Fig. 5). As shown in Fig. 5, most of the S300 particles exhibit irregular shapes, big particles with diameters from 1 to 1.5 μm and small particles with dimensions from 50 to 300 nm are present. All of them aggregate together due to soft aggregate.

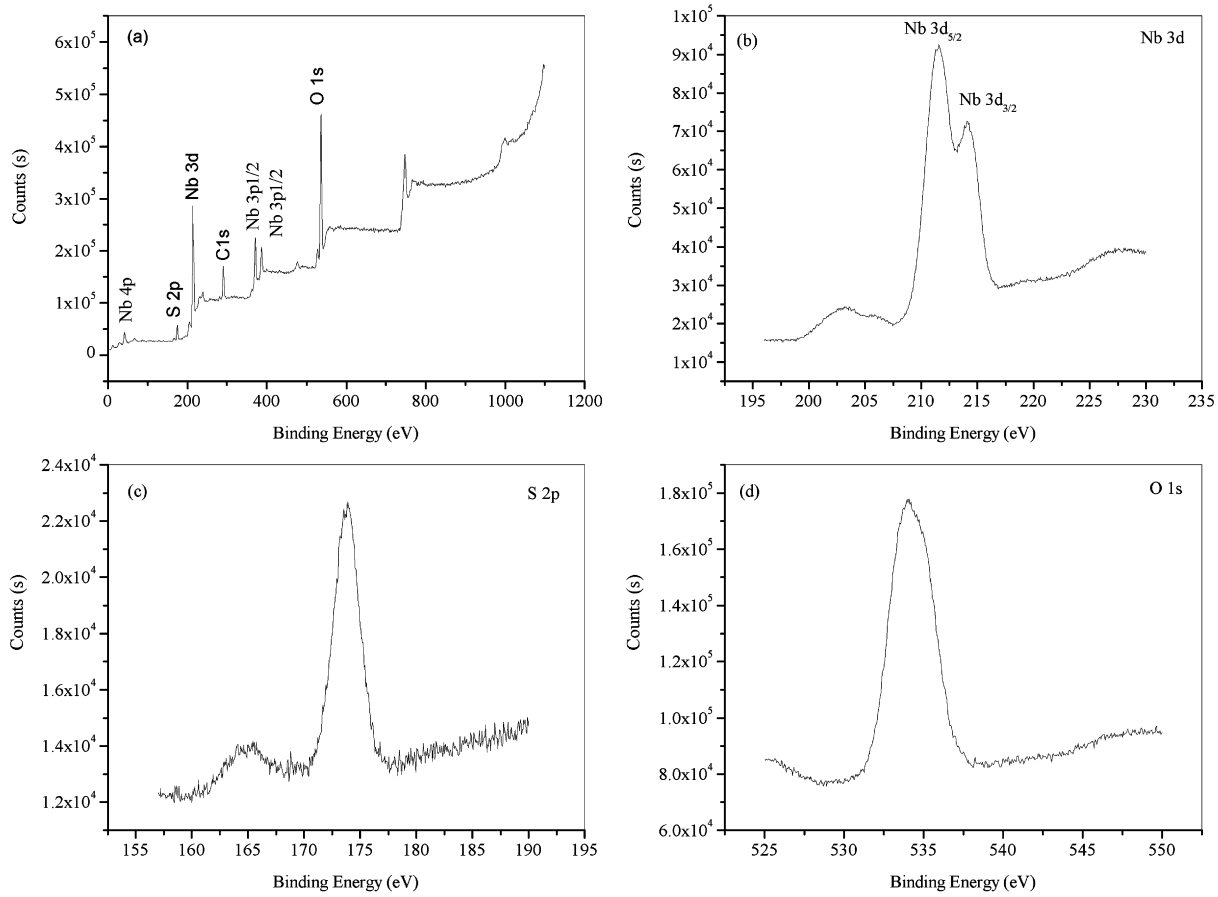

Fig. 8. XPS spectra of S300. (a) Survey spectrum, (b)–(d) detailed spectra of Nb 3d, S 2p and O 1s core levels, respectively.

Table 2
Elemental composition of S300 by EDS (atom%).

Element	O	S	Nb
EDS values	74.95	9.44	15.62
Theoretical values	72.72	9.09	18.18

An EDS spectrum of S300 (coating with platinum on S300 surface) is given in Fig. 6, and the elemental composition is presented in Table 2. It can be seen from Fig. 6 and Table 2 that S300 consists of oxygen (O), sulfur (S) and niobium (Nb). It can be seen from Table 2 that the atomic percentage of each element by EDS is approximately consistent with that of calculated values.

3.1.3. TEM-SAED investigations

Fig. 7 displays the TEM micrograph and the SAED pattern (inset) of S300. It can be observed that the individual grains exhibit sizes in the micron range. The inset of SAED pattern recorded from an individual particle confirms that the S300 is single-crystal and/or multicrystalline.

3.1.4. XPS analysis of S300

Fig. 8(a) shows the XPS survey scan of the niobium oxysulfate, clearly showing the presence of C, S, O and Nb. The existence of C 1s peak is mainly caused by two factors: CO_2 adsorption or carbon compound from environment (contamination carbon). Fig. 8(b) shows the Nb 3d XPS spectra with a double peak structure which is composed of a main peak at 211.5 eV and a satellite peak at 214.0 eV. This doublet is different from the characteristic of Nb—O bonds in Nb_2O_5 [37]. In Fig. 8(c), the peak at 173.9 eV can be assigned to S 2p core level. In Fig. 8(d), the O 1s peak at 534.0 eV suggests that the oxygen exists as O^{2-} species in the $Nb_2O_4(SO_4)$ [38,39].

3.2. Investigation of reaction conditions

3.2.1. Effect of heating temperature

It can be seen from Fig. 9 that the main XRD patterns of the product obtained from the reaction at 200 °C are similar to the standard JCPDs 27-1003 (Nb_2O_5). The XRD features of Nb_2O_5 almost disappear and the product exhibit amorphous phase when the reaction temperature was 250 °C. Crystalline niobium oxysulfate can be obtained and no peaks of Nb_2O_5 are observed when the mixture of H_2SO_4 and Nb_2O_5 was heated at 300 °C.

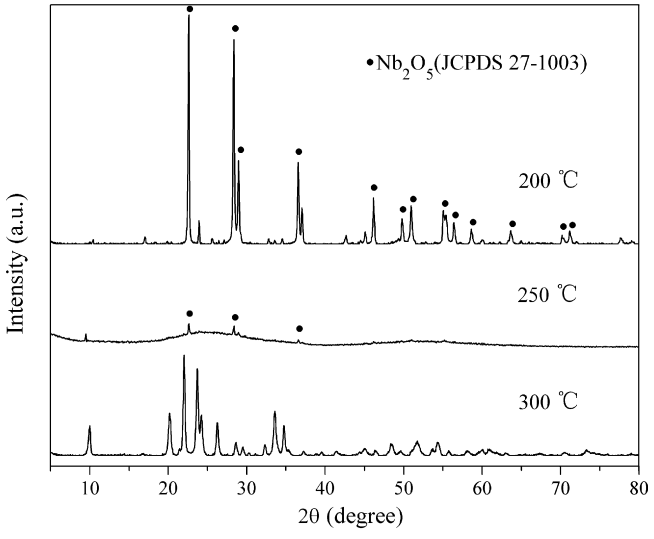

Fig. 9. XRD patterns of the products obtained at different reaction temperatures (H_2SO_4/Nb_2O_5 molar ratio 9.7:1, reaction time 3 h).

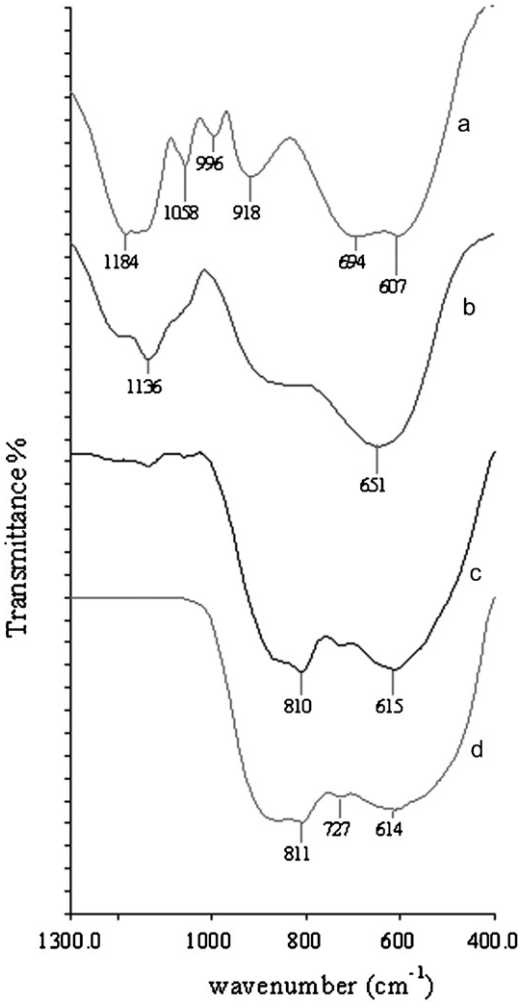

Fig. 10. FTIR spectra of the products obtained at different reaction temperatures: a, 300 °C; b, 250 °C; c, 200 °C; d, pure Nb_2O_5. (H_2SO_4/Nb_2O_5 molar ratio 9.7:1, reaction time 3 h.)

FTIR spectra of the products obtained at different temperatures are presented in Fig. 10. It can be found from Fig. 10c that the peaks in the range from 600 to 850 cm^{-1} correspond with the peaks of Nb_2O_5. These results indicate that almost no reaction occurred between H_2SO_4 and Nb_2O_5 at 200 °C. The characteristic peak of SO_4^{2-} (at 1136 cm^{-1}) can be obviously observed and peaks at 600–850 cm^{-1} broaden when the reaction temperature was 250 °C (Fig. 10b). It can be better explained that a large amount of Nb_2O_5 reacts with H_2SO_4 and most of SO_4^{2-} group with unidentate ligand exists in the product when the mixture is heated at 250 °C. The significant feature of SO_4^{2-} (in the range from 900 to 1200 cm^{-1}) became more apparent when the reaction temperature is increased to 300 °C (Fig. 10a).

3.2.2. Effect of molar ratio of H_2SO_4 to Nb_2O_5

The XRD patterns of the products obtained at different H_2SO_4/Nb_2O_5 molar ratios are given in Fig. 11. It can be seen that the composition and crystal form of the product were unchanged. The molar radio of H_2SO_4 to Nb_2O_5 (4.8:1–120.7:1) does not make any difference for the reaction at 300 °C for 3 h.

3.2.3. Effect of reaction time

The mixture of 40 mL H_2SO_4 and 20 g Nb_2O_5 was heated at 300 °C for 3, 10, and 20 h, respectively. The XRD patterns (Fig. 12)

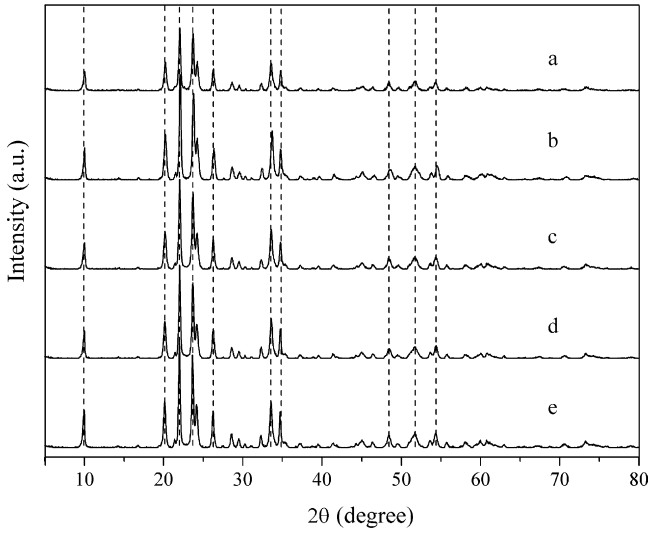

Fig. 11. XRD patterns of the products obtained at different H_2SO_4/Nb_2O_5 molar ratios after heated at 300 °C for 3 h [a, 4.8:1 (20 mL H_2SO_4/20 g Nb_2O_5); b, 7.2:1 (30 mL H_2SO_4/20 g Nb_2O_5); c, 9.7:1 (40 mL H_2SO_4/20 g Nb_2O_5); d, 19.3:1 (40 mL H_2SO_4/10 g Nb_2O_5); e, 120.7:1 (50 mL H_2SO_4/2 g Nb_2O_5)].

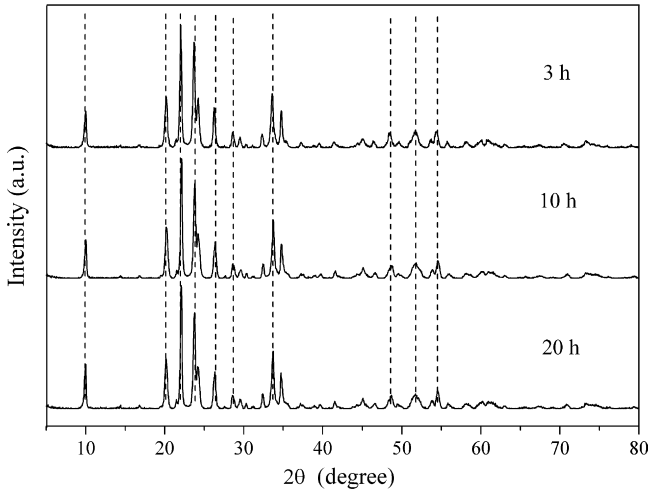

Fig. 12. XRD patterns of the products obtained with different reaction time (H_2SO_4/Nb_2O_5 molar ratio 9.7:1, reaction temperature 300 °C).

demonstrate that the different reaction time has no influence on the composition and crystal structure of the samples.

4. Conclusions

The reaction of Nb_2O_5 with 96% H_2SO_4 is investigated in detail. A different Crystal form of $Nb_2O_4(SO_4)$ is obtained and its thermal stability is studied. It is demonstrated that the optimum reaction temperature is 300 °C for the synthesis of crystalline $Nb_2O_4(SO_4)$ by reacting Nb_2O_5 with 96% H_2SO_4. No differences are observed for the composition and crystal structure of the products when H_2SO_4 and Nb_2O_5 reacted in different molar ratios (4.8:1–120.7:1) and reaction time (3–20 h). The structure resolution by powder XRD reveal that $Nb_2O_4(SO_4)$ crystallizes in the orthorhombic with space group *Pmma* (no. 51) and contains four formula units in the unit cell.

References

[1] X. Wei, L.M. Ye, Y.Z. Yuan, J. Nat. Gas Chem. 18 (2009) 295.
[2] P. Porcher, D.R. Svoronos, M. Leskelä, J. Hölsä, J. Solid State Chem. 46 (1982) 101.
[3] K. Ikeue, T. Kawano, M. Eto, D.J. Zhang, M. Machida, J. Alloys Compd. 451 (2008) 338.
[4] M. Machida, K. Kawamura, K. Ito, K. Ikeue, Chem. Mater. 17 (2005) 1487.
[5] K. Ikeue, M. Eto, D.J. Zhang, T. Kawano, M. Machida, J. Catal. 248 (2007) 46.
[6] M. Machida, K. Kawamura, T. Kawano, D.J. Zhang, K. Ikeue, J. Mater. Chem. 16 (2006) 3084.
[7] D.J. Zhang, F. Yoshioka, K. Ikeue, M. Machida, Chem. Mater. 20 (2008) 6697.
[8] B.M. Casari, V. Langer, J. Solid State Chem. 180 (2007) 1616.
[9] X.T. Sun, T.W. Shi, L. Xiang, W.C. Zhu, Nanoscale Res. Lett. 3 (2008) 386.
[10] M. Shoji, K. Sakurai, J. Alloys Compd. 426 (2006) 244.
[11] T. Kijima, T. Isayama, M. Sekita, M. Uota, G. Sakai, J. Alloys Compd. 485 (2009) 730.
[12] S. Yamamoto, S. Tamura, N. Imanaka, J. Alloys Compd. 418 (2006) 226.
[13] N. Chaiyo, R. Muanghlua, S. Niemcharoen, B. Boonchom, N. Vittayakorn, J. Alloys Compd. 509 (2011) 2445.
[14] S.Y. Lee, C.W. Ahn, J.S. Kim, A. Ullah, H.J. Lee, J. Alloys Compd. 509 (2011) L194.
[15] J. Bellemare, J. Huot, J. Alloys Compd. 512 (2012) 33.
[16] L. Li, G.L. Feng, D.J. Wang, H. Yang, Z.M. Gao, B.X. Li, D.P. Xu, Z.H. Ding, X.Y. Liu, J. Alloys Compd. 509 (2011) L263.
[17] H.T. Wu, L.X. Li, Q. Zou, Q.W. Liao, P.F. Ning, P. Zhang, J. Alloys Compd. 509 (2011) 2232.
[18] F. Rubio-Marcos, P. Marchet, X. Vendrell, J.J. Romero, F. Rémondière, L. Mestres, J.F. Fernández, J. Alloys Compd. 509 (2011) 8804.
[19] C.L. Huang, Y.H. Chien, J. Alloys Compd. 509 (2011) L293.
[20] M.K. Suresh, A. John, J.K. Thomas, P.R.S. Wariar, S. Solomon, J. Alloys Compd. 509 (2011) 2401.
[21] N. Li, W.L. Li, L.D. Wang, S.Q. Zhang, J.W. Ye, W.D. Fei, J. Alloys Compd. 509 (2011) 8028.
[22] D. Kajewski, Z. Ujma, J. Alloys Compd. 509 (2011) 7532.
[23] J.H. Park, Y.J. Choi, S. Nahm, J.G. Park, J. Alloys Compd. 509 (2011) 6908.
[24] H.F. Zhai, X. Qian, J.Z. Kong, A.D. Li, Y.P. Gong, H. Li, D. Wu, J. Alloys Compd. 509 (2011) 10230.
[25] Y.L. Li, C. Hui, Y.X. Li, Y.L. Wang, J. Alloys Compd. 509 (2011) L203.
[26] J.E. Land, J.R. Sanchez-Caldas, J. Less-Common Met. 13 (1967) 233.
[27] Y.G. Goroshchenko, J. Inorg. Chem. USSR (English Trans.) 1 (1956) 24.
[28] Y.G. Goroshchenko, M.I. Andreeva, Russ. J. Inorg. Chem. 8 (1963) 505.
[29] M. Boström, M. Gemmib, W. Schnelle, J. Solid State Chem. 177 (2004) 1738.
[30] B. Ewald, Yu Prots, Z. Kristallogr. NCS 89 (2004) 219.
[31] U. Betke, M.S. Wickleder, Inorg. Chem. 50 (2011) 858.
[32] M. Ra'ad, Al-Shukry, J. Fadhil, Thermochim. Acta 41 (1980) 281.
[33] K. Nakamoto, Infrared and Raman Spectra of Inorganic and Coordination Compounds, 4th ed., Wiley, New York, 1986.
[34] R.L. parfitt, R.S.C. Smart, J. Chem. Soc. Faraday Trans. I 73 (1977) 766.
[35] R.A. Schoonheydt, J.H. Lunsford, J. Catal. 26 (1972) 261.
[36] R. Eskenazi, J. Raskovan, R. Levitus, J. Inorg. Nucl. Chem. 28 (1966) 521.
[37] R. Romero, J.R. Ramos-Barrado, F. Martin, D. Leinen, Surf. Interface Anal. 36 (2004) 888.
[38] R. Li, X.Y. Tao, X.D. Li, J. Mater. Chem. 19 (2009) 983.
[39] R. Li, L.H. Bao, X.D. Li, CrystEngComm 13 (2011) 5858.